1

Scaling theories of diffusion-controlled and ballistically controlled bimolecular reactions

Sidney Redner

Basic features of the kinetics of diffusion-controlled two-species annihilation, $A+B \to 0$, as well as that of single-species annihilation, $A+A \to 0$, and coalescence, $A+A \to A$, under diffusion-controlled and ballistically controlled conditions, are reviewed in this chapter. For two-species annihilation, the basic mechanism that leads to the formation of a coarsening mosaic of A- and B-domains is described. Implications for the distribution of reactants are also discussed. For single-species annihilation, intriguing phenomena arise for 'heterogeneous' systems, where the mobilities (in the diffusion-controlled case) or the velocities (in the ballistically controlled case) of each 'species' are drawn from a distribution. For such systems, the concentrations of the different 'species' decay with time at different power-law rates. Scaling approaches account for many aspects of the kinetics. New phenomena associated with discrete initial velocity distributions and with mixed ballistic and diffusive reactant motion are discussed. A scaling approach is outlined to describe the kinetics of a ballistic coalescence process which models traffic on a single-lane road with no passing allowed.

1.1 Introduction

There are a number of interesting kinetic and geometric features associated with diffusion-controlled two-species annihilation, $A + B \to 0$, and with single-species reactions, $A + A \to 0$ and $A + A \to A$, under diffusion-controlled and ballistically controlled conditions.

In two-species annihilation, there is a spontaneous symmetry breaking in which large-scale single-species heterogeneities form when the initial concentrations of the two species are equal and spatially uniform. Underlying this domain formation is an effective repulsion between A and B that favors seg-

regation of particles into single-species domains. In low spatial dimension, this effective repulsion dominates over the mixing due to diffusion. The resulting spatial organization invalidates the mean-field approximation and its corresponding predictions. Scaling approaches provide an understanding for the origin of this spatial organization and some of its consequences. Related ideas can be applied to the situation where the reactants move by driven diffusive motion, the particles hopping in only one direction. Counter to naive intuition based on Galilean invariance, the reaction kinetics with driven diffusion is qualitatively different from that which occurs with isotropic diffusion and hard-core repulsion.

While single-species reactions are fundamentally simpler than two-species annihilation, there is a wide range of phenomenology that is not fully explored. For example, the 'heterogeneous' single-species reaction, where each reactant moves at a different rate, naturally raises new questions regarding the relation between the initial mobility distribution and the decay rate of different mobility 'species'. These issues are more central when particles move ballistically, so that the initial condition is the only source of stochasticity in the system. In spite of this simplicity, rich and unanticipated phenomena occur, especially for a discrete initial velocity distribution. The case of $A + A \to 0$ with combined diffusive and ballistic motion is particularly surprising because the concentration decay in this composite process is faster than that of the reaction with only ballistic motion or only diffusion. This intriguing behavior can be understood through dimensional analysis. Finally, in ballistically driven aggregation, $A_i + A_j \to A_{i+j}$, scaling arguments can be advantageously combined with analytic methods to give a comprehensive account of the kinetics in a momentum-conserving process and in a model that mimics traffic flow on a single-lane road.

In Sec. 1.2, the primary features that characterize the kinetics and spatial organization in two-species annihilation are outlined. The emphasis is on qualitative approaches that should be applicable to many nonequilibrium phenomena. This section closes with a (necessarily incomplete) outline of recent and not fully understood results for $A + B \to 0$ with driven diffusive reactant motion. Section 1.3 is devoted to single-species reactions. In spite of the wide diversity of phenomena, scaling analyses for time-dependent population distributions provide unifying and comprehensive descriptions of the kinetics. A number of case studies are presented, with mention of some open questions in addition to discussions of known results. A brief summary is given in Sec. 1.4.

1.2 Diffusion-controlled two-species annihilation

In diffusion-limited two-species annihilation, an intriguing aspect of the kinetics is that the density decays more slowly than the rate equation (mean-field) prediction of $1/t$, for a random initial condition of reactants with equal densities for the two species. This fundamental observation, first made by Zel'dovich and coworkers [1] and independently rediscovered by Toussaint and Wilczek [2], stimulated considerable interest and continues to foster current research [3-11]. To appreciate the basic issues, a mean-field description of the decay kinetics in single species reactions is outlined in the next subsection. A heuristic approach for the kinetics of two-species annihilation, which is based on the existence of large-scale spatial heterogeneity, is then presented.

1.2.1 Preliminary: mean-field theory for single-species reactions

In the single-species reaction, irreversible annihilation occurs whenever two particles approach within a reaction radius R. To determine the decay of the concentration within a mean-field approximation, note that in a time of order $1/c$, where $c \equiv c(t)$ is the concentration, each particle will typically encounter another particle. Consequently, in a time $\Delta t \propto 1/kc$, where k is the reaction rate, the concentration decrement, Δc, will be of order c. Combining these gives the mean-field rate equation,

$$\dot{c} \cong \Delta c/\Delta t \propto -kc^2, \tag{1.1}$$

with solution $c(t) = c(0)/[1 + c(0)\,kt] \sim (kt)^{-1}$. Thus the exponent of the power-law decay is -1, and the time scale is set by k. As discussed below, this exponent value is correct only for spatial dimension $d \geq 4$, the regime of validity of the mean-field approach.

It is instructive to determine the scaling of the reaction rate k [2]. By dimensional analysis of (1.1), k has units $[\ell]^d/[t]$. Furthermore, k is a function only of the diffusion coefficient, D, and the particle radius, R. The only combination of these quantities that possesses the correct units is

$$k \propto DR^{d-2}. \tag{1.2}$$

For $d > 2$, this ansatz agrees with the Smoluchowski theory [12], in which the reaction rate is given by the steady-state flux towards an absorbing test particle due to the remainder of the particles in the system. However, for $d < 2$, (1.2) leads to the nonsensical conclusion that the reaction rate decreases with increasing particle radius. To determine the appropriate behavior for $d < 2$,

one can still apply the Smoluchowski theory, but its interpretation must be modified. Because the incident flux is time dependent, even as $t \to \infty$, the reaction rate now acquires a time dependence of the form $k \propto D^{d/2}/t^{1-d/2}$ for $d < 2$ and $k \propto D/\ln Dt$ for $d = 2$. The lack of dependence on the particle radius is a manifestation of the recurrence of random walks [13] for $d \leq 2$. Therefore, with respect to diffusion, the collision radius is effectively infinite and thus drops out of the system. Employing these reaction rates in the rate equation gives the asymptotic behaviors appropriate for $d \leq 2$:

$$c(t) \propto (Dt)^{-d/2}, \quad d < 2; \qquad c(t) \propto (\ln Dt)/Dt, \quad d = 2. \tag{1.3}$$

These results can also be obtained from a more microscopic, but equally nonrigorous approach. Because of the recurrence of random walks for $d \leq 2$, the time for a particular reaction to occur should be of order $\Delta t \propto \ell^2/D$, where $\ell \propto c^{-1/d}$ is the typical interparticle spacing. In this formulation, the reaction rate does not enter in the collision time because random walk trajectories are compact. Therefore if two reactants collide once, they will collide an infinite number of times and the reaction rate rescales to a large value. Consequently, for $d < 2$ the rate equation becomes

$$\dot{c} \cong \Delta c/\Delta t \propto -\left(c/D^{-1}c^{-2/d}\right) = -Dc^{1+2/d}, \tag{1.4}$$

with solution $c(t) \sim (Dt)^{-d/2}$. A straightforward adaptation of this approach also gives a logarithmic correction for the case $d = 2$. Notice that for $d = 1$ the above mean-field approaches give either $\dot{c} \propto -c^2/\sqrt{t}$ or $\dot{c} \propto -c^3$ for the 'effective' rate equation. Both give the correct decay of the concentration, but neither can be rigorously justified. In fact, from the exact solution in one dimension, it may be appreciated that a polynomial rate equation is inadequate in many respects [14], even though it can be engineered to reproduce the correct exponents.

1.2.2 Fluctuation-driven kinetics in two-species annihilation

For $d \leq 4$, the above embellishments of the rate equation are inadequate because single-species domains form, thus invalidating the homogeneity assumption implicit in the mean-field approach. The long-time behavior of $c(t)$ can be understood from the following account of local density fluctuations. Roughly speaking, the difference in the number of A's and B's in a finite volume of linear dimension L remains nearly constant during the time for a particle to traverse the volume by diffusion, $t_L \sim L^2/D$. At $t = 0$, this difference is of the order of the square root of the initial particle number: $N_A - N_B \approx \pm\sqrt{c(0)}\, L^{d/2}$. After a time t_L has elapsed, only the local

majority species remains in the domain, whose number $N_>(t_L)$ is of order $\sqrt{c(0)}\, L^{d/2}$. Elimination of L in favor of t gives

$$c(t) \approx N_>(t)/L^d \sim \sqrt{c(0)}\, (Dt)^{-d/4}, \qquad d \leq 4. \tag{1.5}$$

Thus a homogeneous system evolves into a continuously growing domain mosaic whose individual identities are determined by the local majority species in the initial state. At time t, these domains will be of typical linear dimension $\sqrt{Dt}$, within which a single species of concentration $\sqrt{c(0)}\, (Dt)^{-d/4}$ remains.

However, for $d > 4$ the domains are unstable and mean-field theory applies. To justify this consider, for example, the fate of an A particle inside a B domain of linear dimension L and local concentration $\sim L^{-d/2}$. The impurity needs L^2 time steps to exit the domain, during which L^2 distinct sites will have been visited. At each site, the A particle will react with a probability of the order of the B concentration, $L^{-d/2}$. Therefore the probability that an A particle is unsuccessful in exiting a B domain is of order $L^{(4-d)/2}$. Since this vanishes as $L \to \infty$ if $d > 4$, a growing domain mosaic is eventually unstable to diffusive homogenization for $d > 4$.

1.2.3 Multiple microscopic lengths

The above arguments indicate that two lengths characterize the reactant distribution in 1D: the average domain size $L \propto (Dt)^{1/2}$ and the typical interparticle spacing, which scales as $c(t)^{-1} \propto t^{1/4}$. A surprising feature, which reveals a richer structure for the reactant distribution, is that the typical distances between AA and AB closest-neighbor pairs, ℓ_{AA} and ℓ_{AB}, grow with different powers of time for $d < 3$ [15]. The latter characterizes the interdomain 'gap' that separates adjacent domains (Fig. 1.1). This gap controls the kinetics, since each reaction event involves diffusion of an AB pair across a gap. The different scalings of ℓ_{AA} and ℓ_{AB} indicate that nontrivial modulation exists in the reactant concentration over the extent of a domain.

To determine the evolution of ℓ_{AB} in 1D, consider the time dependence of the concentration of closest-neighbor AB pairs, c_{AB}. Typical AB pairs react in a time $\Delta t \sim \ell_{AB}^2/D$. Since the number of reactions per unit length is of order c_{AB}, the time rate of change of the overall concentration is

$$\Delta c/\Delta t \approx -c_{AB} \Big/ \left(\ell_{AB}^2/D\right). \tag{1.6}$$

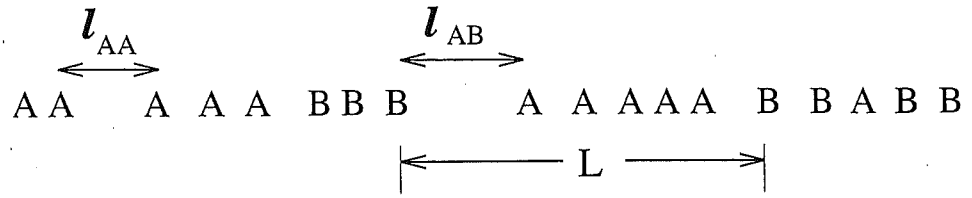

Fig. 1.1. Definition of fundamental interparticle distances in 1D: the typical distance between closest-neighbor same species particles, ℓ_{AA}, the distance between closest-neighbor unlike species, ℓ_{AB}, i.e., the gap between domains, and the typical domain length, L.

The l.h.s. is known from $c(t)$ itself, while in 1D $c_{AB} \propto (Dt)^{-1/2}$, since there is one AB pair per domain of typical size $(Dt)^{1/2}$. These give

$$\ell_{AB} \propto c(0)^{-1/4}\,(Dt)^{3/8}. \tag{1.7}$$

Thus at least three lengths characterize the reactant distribution: in addition to the average domain size and the typical interparticle spacing, there is the interdomain gap $\ell_{AB} \propto t^{3/8}$. The inequality $\ell_{AB} \gg \ell_{AA}$ is a manifestation of the effective repulsion between opposite species.

The above results can be generalized to spatial dimension $1 \leq d \leq 2$. The time dependence of ℓ_{AB} still follows by applying (1.6), since it holds whenever random walks are compact. Under the assumption of a smooth domain perimeter of linear dimension $t^{(d-1)/2}$ and particles in the perimeter zone separated by a distance of the order of ℓ_{AB}, irrespective of identity, it is straightforward to obtain

$$\ell_{AB} \propto t^{\frac{(d+2)}{4(d+1)}}, \qquad c_{AB}(t) \propto t^{-\frac{d(d+3)}{4(d+1)}}, \tag{1.8}$$

which gives $\ell_{AB} \sim t^{1/3}$ and $c_{AB}(t) \sim t^{-5/6}$ for $d = 2$. For $d > 2$, the transience of random walks implies that two opposite-species particles within a region of linear dimension ℓ_{AB} will react in a time of order ℓ_{AB}^d (rather than ℓ_{AB}^2). Consequently, (1.6) should be replaced by $\Delta c/\Delta t \approx -c_{AB}/\ell_{AB}^d$. This relation, together with the assumption of a smooth interfacial region between domains, gives, for $d > 2$,

$$\ell_{AB} \approx t^{\frac{d+2}{4(2d-1)}}, \qquad c_{AB} \approx t^{-\frac{d^2+5d-4}{4(2d-1)}}. \tag{1.9}$$

These coincide with (1.8) at $d = 2$, but yield $c_{AB} \approx t^{-1}$ and $\ell_{AB} \approx t^{1/4}$ for $d = 3$. The latter represents the limit at which ℓ_{AB} is of the same order as ℓ_{AA}. Thus the nontrivial scaling of interparticle distances disappears in three dimensions and above.

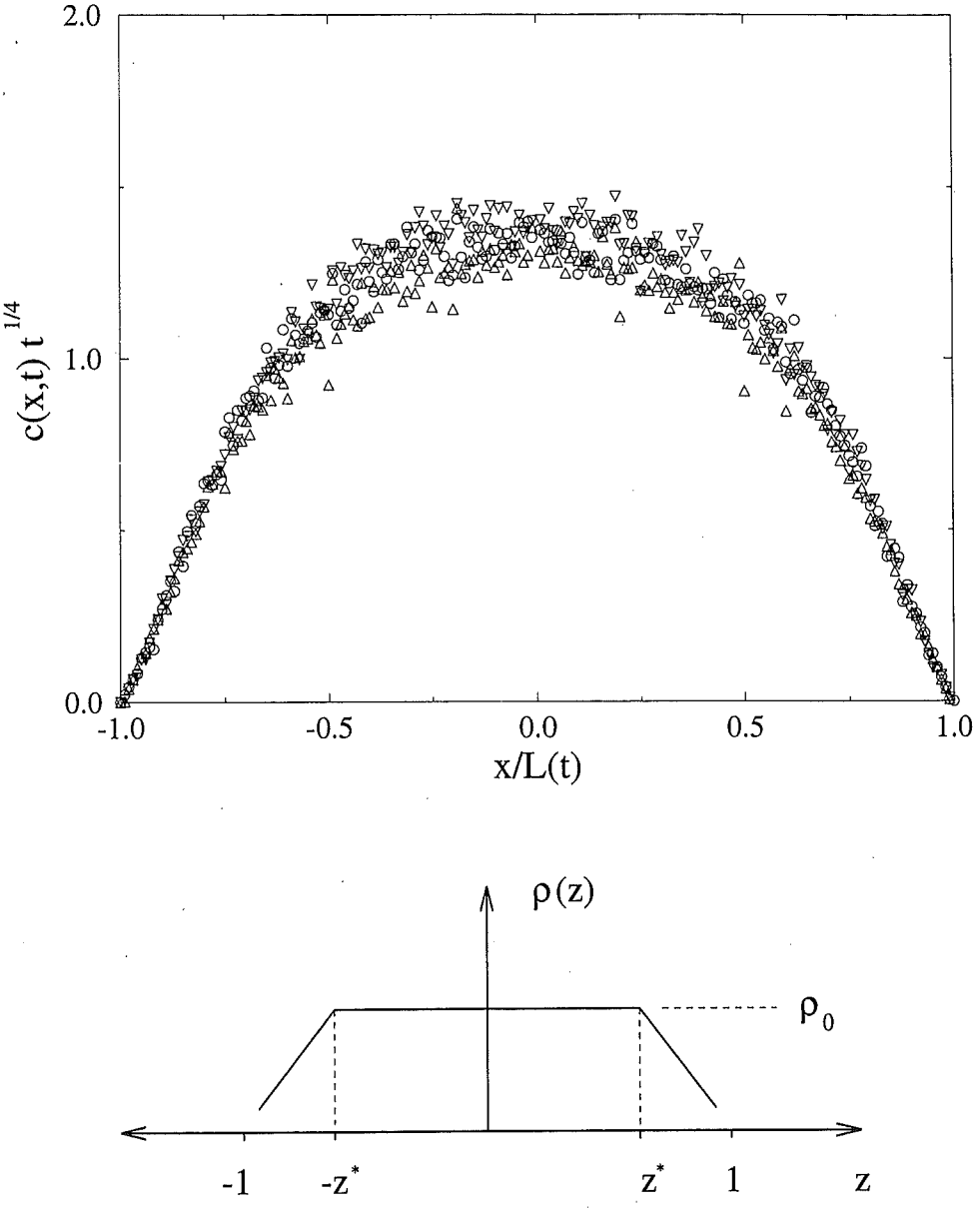

Fig. 1.2. (a) Simulation data for the scaled microcanonical density profile of a single domain, for $A + B \to 0$ with isotropic diffusion, at $t = 1.5^{13} \cong 194$ ($\triangle$), $t = 1.5^{18} \cong 1477$ ($\triangledown$), and $t = 1.5^{23} \cong 11222$ (o). Plotted is the scaled local concentration, $\rho(z) \equiv c(x,t)\,t^{1/4}$ (in arbitrary units) *vs.* $z \equiv x/L(t)$. Here $\pm L(t)$ defines the extent of the domain, and x is a local coordinate with respect to the center of the domain. (b) Idealized trapezoidal form. In the domain core the density is relatively constant, while the density vanishes linearly as a function of the distance to the domain edge.

1.2.4 Domain profile and interparticle distance distribution

A revealing picture of the reactant distribution is obtained from the average concentration of a single domain [15]. Consider the 'microcanonical' density profile, $P^{(M)}(x)$, defined as the probability of finding a particle at a scaled distance x from the domain midpoint when each domain is first scaled to a *fixed* size (Fig. 1.2(a)). The resulting distribution is similar to the long-time probability distribution for pure diffusion in a fixed-size absorbing domain. In contrast, for two-species annihilation, particles in a single domain are confined by absorbing boundaries that recede stochastically as $\sqrt{t}$ —the typical domain size. While the probability distribution inside such a stochastically evolving domain has not been solved, one can solve the related problem of a particle inside a deterministically growing domain $[-L(t), L(t)]$ with $L(t) \propto t^{1/2}$. The adiabatic approximation marginally applies in this case [16], and the density profile has the form $\cos[\pi x/L(t)]$. This simple-minded modeling provides a useful framework for understanding the domain profile in the reacting system.

Although determined by interactions between *opposite* species, this inhomogeneous domain profile governs the distribution of interparticle distances between the *same* species. Particles are typically separated by a distance that grows as $t^{1/4}$ within the core of the domain, but systematically become sparser as the domain interface is approached. The subregions of 'core' and 'interface' each comprise a finite fraction of the domain. These essential features of the profile may be accounted for by a trapezoidal form, Fig. 1.2(b),

$$\rho(z) \equiv c(x,t)\, t^{1/4} = \begin{cases} \rho_0, & |z| \le z^*; \\ \rho_0(1-|z|), & z^* < |z| < 1-\epsilon. \end{cases} \tag{1.10}$$

Here $z \equiv x/L(t)$ is the scaled spatial coordinate, where $x \in [-L(t), L(t)]$, and ρ_0 and $z^* \lesssim 1$ are constants. The upper limit for $|z|$ in the second line of (1.10) reflects the fact that there are no particles within a scaled distance of $\epsilon \equiv \ell_{AB}/L(t) \sim t^{-1/8}$ from the domain edge. The linear decay of the concentration near the domain edge arises from the finite flux of reactants that leave the domain. Thus, the local nearest-neighbor distance is $\rho(z)^{-1}$, where $\rho(z) = \rho_0$ in the core ($|z| \le z^*$), and $\rho(z) = \rho_0(1-|z|)$ near the boundary; the time dependence of the reduced moments of the AA distance distribution are then

$$M_n \equiv \langle \ell_{AA}^n \rangle^{1/n} = \left(\int_0^\infty x^n \, P_{AA}(x,t)\, dx \right)^{1/n}$$
$$\approx t^{1/4} \left(2 \int_0^{z*} \frac{dz}{\rho_0^n} + 2 \int_{z*}^{1-\epsilon} \frac{dz}{\rho_0^n (1-z)^n} \right)^{1/n}$$
$$\sim \begin{cases} t^{1/4}, & n < 1; \\ t^{1/4} \ln t, & n = 1; \\ t^{(3n-1)/8n}, & n > 1. \end{cases} \tag{1.11}$$

For $n < 1$, the dominant contribution to M_n originates from the ρ_0^{-n} term in the parentheses, while for $n \geq 1$ the term involving $\rho_0^{-n}(1-z)^{-n}$ dominates, the second term giving a logarithmic singularity at the upper limit for $n = 1$. Thus the large-scale modulation in the domain profile leads to moments $M_n(t)$ that are governed by both the gap lengths, ℓ_{AB} and ℓ_{AA}. As $n \to \infty$, the reduced moment is dominated by the contribution from the sparsely populated region near the domain periphery where nearest-neighbor particles are separated by a distance of order $t^{3/8}$.

1.2.5 Driven diffusive motion

A recent surprising development has been the discovery by Janowsky [17] that the concentration decays as $t^{-1/3}$ when particles move by driven diffusion. In this mechanism, each particle attempts to move only to the right and actually moves only if the target site is at that instant unoccupied by a particle of the same species. If the incident particle lands on a site already occupied by an opposite species particle, annihilation occurs. By Galilean invariance, one might anticipate that $c(t) \propto t^{-1/4}$, as in $A + B \to 0$ with isotropic diffusion and with the same hard-core exclusion.

A rough argument for the $t^{-1/3}$ decay with driven diffusion follows from a description of the dynamics of a single AB interface [18] using the continuum inviscid Burgers' equation. Consider the 'separated' initial condition with $c_A(x, t = 0) = \overline{c}_A \Theta(-x)$ and $c_B(x, t = 0) = \overline{c}_B \Theta(x)$, where $\Theta(x)$ is the Heaviside step function. By applying mass balance as the interface moves, one finds that the interfacial velocity is the following function of the initial densities:

$$v_{AB} = \begin{cases} 1 - 2\,\overline{c}_B(\sqrt{2}-1), & \overline{c}_A \geq \overline{c}_B(\sqrt{2}-1); \\ 1 - (\overline{c}_A^2 + \overline{c}_B^2)\,/\,(\overline{c}_A + \overline{c}_B), & \overline{c}_A < \overline{c}_B(\sqrt{2}-1). \end{cases} \tag{1.12}$$

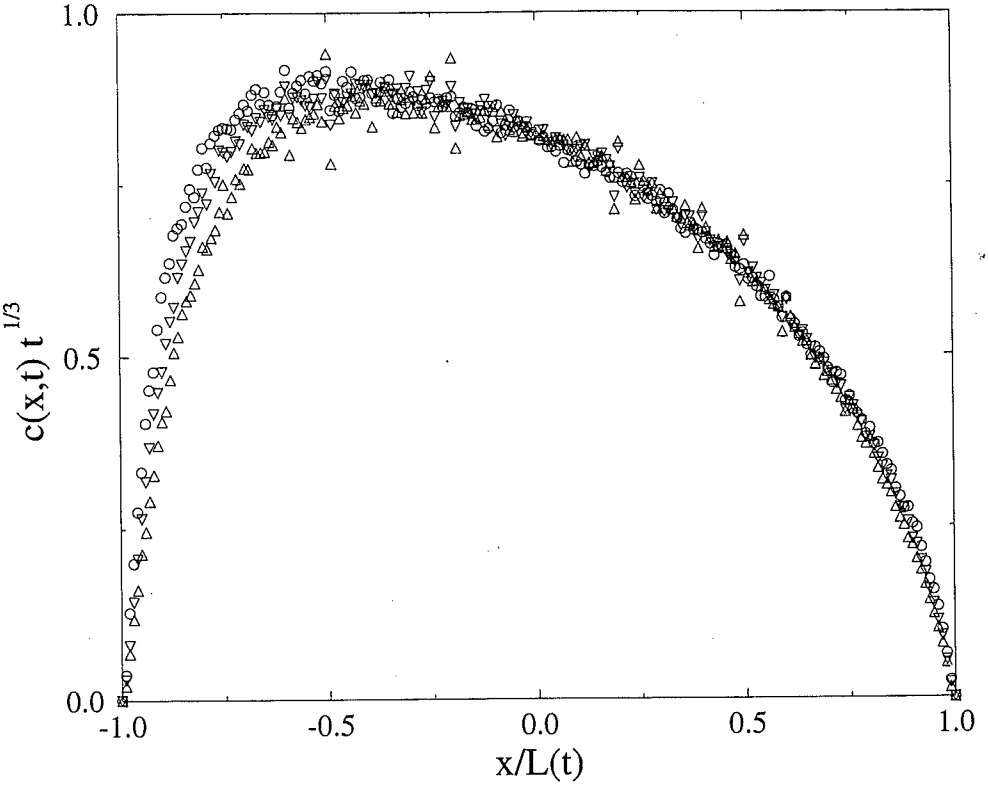

Fig. 1.3. Simulation data for the scaled microcanonical density profiles for $A+B \to 0$ with driven diffusive motion at $t = 1.5^{17} \cong 985$ ($\triangle$), $t = 1.5^{20} \cong 3325$ ($\triangledown$), and $t = 1.5^{23} \cong 11222$ (o). Plotted is the scaled local concentration, $c(x,t)\,t^{1/3}$ (in arbitrary units) *vs.* $x/L(t)$.

For a random, equal-density, initial condition, this leads to a domain length growing as $dL/dt \propto |v_{AB} - v_{BA}|$, which from (1.12) is proportional to the density difference across the interfaces. These differences are typically of the order of the domain densities themselves, leading to $dL/dt \propto c_{AB} - c_{BA} \propto c(t)$. Since the typical concentration in a domain of length L is of order $1/\sqrt{L}$, the domain size should therefore grow as $L \sim t^{2/3}$, while the concentration should decay as $c(t) \sim t^{-1/3}$.

A more microscopic description emerges from the scaled microcanonical domain profile in which the length is rescaled by $t^{-2/3}$ and the density by $t^{1/3}$ (Fig. 1.3). This profile exhibits good data collapse over most of the domain, except near the trailing edge. The departure from 'bulk' scaling appears to stem from diffusive boundary layers of size $\sqrt{t}$. The relative extent of this boundary layer with respect to the domain length decreases as $t^{-1/6}$, in qualitative agreement with numerical simulations. Janowsky

[19] has recently obtained similar results for the domain profile, but gives a somewhat different interpretation.

1.3 Single-species reactions

The kinetics of *homogeneous* diffusion-controlled single-species annihilation, $A + A \to 0$, and coalescence, $A + A \to A$, is now relatively well understood. For spatial dimension $d > 2$, the kinetics is accounted for by the rate equation, which predicts that $c(t) \propto t^{-1}$. For $d \leq 2$, suitably modified rate equations and the Smoluchowski approach both predict that $c(t) \propto t^{-d/2}$, but with logarithmic corrections appearing for $d = 2$. In 1D, exact solutions, based on the image method [20], an occupation number formalism [21], or a mapping onto the kinetic Ising-Glauber model at zero temperature [22] provide definitive results for single-species annihilation. Accompanying the anomalous kinetics for $d \leq 2$ is a spatial 'ordering' in which the probability of finding particles at the typical separation is enhanced compared to a random distribution [14,23]. Similarly, for diffusion-controlled coalescence, exact solutions have been constructed based on analyses of interparticle distribution functions [14] or on analogies with the voter model [24] and related probabilistic formulations [25-27].

1.3.1 Heterogeneous diffusive motion

A generalization of single-species annihilation that exhibits a wide range of phenomenology is *heterogeneous* annihilation, $A_i + A_j \xrightarrow{K_{i,j}} 0$ [28]. Here A_i denotes the ith 'species', with diffusivity D_i, and the reaction rate matrix $K_{i,j}$ is a function of the diffusivities of the two reacting 'species'; we use the terminology of different species to describe a reaction that is actually single-species annihilation but with distinct rates for different reaction channels. This simple generalization has a surprisingly rich array of kinetics.

The rate equations can be adapted to account for the kinetics in the mean-field approximation. When the number of species is finite, the rate equations predict that the least mobile species decays as t^{-1}, while the other species decay more quickly, each with an associated exponent that depends on the diffusivity ratio between it and the slowest species.

When the diffusivities are drawn from a continuous distribution, the evolution of the diffusivity distribution, $P(D,t)$, is described by the integro-

differential equation

$$\frac{\partial P(D,t)}{\partial t} = -P(D,t)\int_0^\infty dD'\,(D+D')\,P(D',t)$$
$$= -P(D,t)[D\,\mathcal{P}_0(t)+\mathcal{P}_1(t)], \qquad (1.13)$$

where the kth moment $\mathcal{P}_k(t) \equiv \int_0^\infty dD\,D^k\,P(D,t)$. Thus the zeroth moment gives the particle concentration, $c(t) = \mathcal{P}_0(t)$, while the average diffusion coefficient $\langle D\rangle = \mathcal{P}_1(t)/\mathcal{P}_0(t)$. The solution to (1.13) is

$$P(D,t) = P(D,0)\exp\left[-D\int_0^t \mathcal{P}_0(t')dt' - \int_0^t \mathcal{P}_1(t')dt'\right]$$
$$= P(D,0)\,\sqrt{\mathcal{P}_0(t)}\,\exp\left[-D\int_0^t c(t')dt'\right], \qquad (1.14)$$

where the second line is obtained by first integrating (1.13) over D to relate the moments $\mathcal{P}_1$ and $\mathcal{P}_0$.

When $P(D,t=0) \sim D^\mu$ as $D \to 0$, (1.14) can be analyzed by scaling. Under the assumption of power-law decays for the average concentration and diffusivity, $c \sim t^{-\alpha}$ and $\langle D\rangle \sim t^{-\beta}$ for $t \to \infty$, a natural scaling ansatz for the time-dependent diffusivity distribution is

$$P(D,t) \simeq t^{\beta-\alpha}\Phi(Dt^\beta). \qquad (1.15)$$

Substituting this into (1.14) and applying consistency conditions, one finds [28] the basic exponents to be $\alpha = (2+2\mu)/(3+2\mu)$, $\beta = 1/(3+2\mu)$.

For $d \leq 2$, the Smoluchowski theory [12] is ideally suited for adaptation to heterogeneous $A_i + A_j \to 0$. As outlined in Sec. 1.2, in the Smoluchowski approach one computes the particle flux towards a reference absorbing particle of the rest of the background particles. In 1D, this background concentration is $c(x,t) = c_\infty\,\mathrm{erf}(x/\sqrt{4Dt})$, from which the particle flux to the absorber is $\phi = c_\infty\sqrt{D/\pi t}$. This is identified as an *effective* reaction rate, $\tilde{k}$.

As an illustrative and intriguing example, consider the 'impurity' problem, namely a background of identical particles with diffusivity D and concentration c, and relatively rare impurities of diffusivity D_I and concentration c_I in 1D. In 1D, the survival of an impurity is equivalent to the probability that a given Ising spin with zero-temperature Glauber dynamics does not flip. This specific problem has been raised in studies of domain-coarsening phenomena [29]. In the limit of $c_I \ll c$, the influence of background-impurity and impurity-impurity reactions can be neglected and the effective (Smoluchowski)

rate equations are

$$\dot{c} \cong -2\tilde{k}_{BB}c^2 \sim -2\sqrt{\frac{2D}{\pi t}}c^2, \quad \dot{c}_I \cong -2\tilde{k}_{BI}cc_I \sim -2\sqrt{\frac{D+D_I}{\pi t}}cc_I. \quad (1.16)$$

Here $\tilde{k}_{BB}$ and $\tilde{k}_{BI}$ are the effective rates for background-background and background-impurity reactions, obtained from straightforwardly generalizing the Smoluchowski theory to particles with different diffusivities. From the first equation, the background concentration vanishes as $c = \sqrt{\pi/(32Dt)}$. (In comparison, $c(t)/c_{\text{exact}}(t) = \pi/2$.) A crucial element of the second equation is that the decay exponent of the impurity species is determined by the *amplitude* of $c(t)$. One finds $c_I(t) \sim t^{-\sqrt{(1+\epsilon)/8}}$, with $\epsilon = D_I/D$.

The special case of the stationary impurity ($\epsilon = 0$) merits emphasis. The above Smoluchowski theory gives the exponent of $c_I(t)$ as $1/\sqrt{8} \cong 0.35355\ldots$, while numerical simulations give 0.375 [28,29]. By a mapping to steady-state aggregation with a point monomer source, Derrida *et al.* [30] have recently shown that this exponent is, in fact, equal to 3/8. An intuitive understanding of this result is still lacking.

The nonuniversal behavior for the impurity decay has a counterpart in single-species coalescence. The impurity decay in coalescence can be simply analyzed, since the 'cage' enclosing a given impurity, defined as its nearest neighbors, evolves *only* by diffusion [31]. This three-body system of the impurity and its two nearest-neighbors can be transformed, in turn, to a single random walker that diffuses within an absorbing two-dimensional wedge whose opening angle depends on D/D_I. This gives a survival probability that decays as $t^{-\alpha}$, with $\alpha = \pi/\{2\cos^{-1}[\epsilon/(1+\epsilon)]\}$.

Such a rigorous mapping does not exist for impurity decay in annihilation, since the cage's evolution is an intrinsically many-body process. Nevertheless, the Smoluchowski theory is qualitatively identical for both annihilation and coalescence. In both cases, the mechanism underlying the nonuniversal impurity decay is the equivalence to the survival probability $S(t)$ of a diffusing particle inside an absorbing interval of length $L = (At)^{1/2}$. For this probability, we have $S(t) \propto t^{-\alpha(A/D)}$, i.e., the decay exponent is dependent on the dimensionless parameter A/D [32]. The Smoluchowski theory predictions turn out (fortuitously perhaps) to be quantitatively accurate for impurity decay in annihilation, but somewhat less accurate in the corresponding coalescence process. For both cases, however, the Smoluchowski approach provides a useful paradigm for treating this nonuniversal aspect of the decay kinetics.

One can also adapt the Smoluchowski approach to heterogeneous annihilation in 1D by incorporating a time-dependent reaction rate in the rate equation (1.13). This leads to

$$\frac{\partial P(D,t)}{\partial T} = -P(D,t)\int_0^\infty dD'\sqrt{D+D'}\,P(D',T). \qquad (1.17)$$

The correspondence with the mean-field approach has been sharpened by introducing the modified variable $T = 4\sqrt{t/\pi}$, to eliminate the time dependence on the r.h.s. of (1.17). While this equation does not appear to be solvable, presumably exact exponent values can be obtained by replacing the kernel by one with the same homogeneity degree, $\sqrt{D+D'} \to \sqrt{D}+\sqrt{D'}$, for which a scaling analysis yields the exponents $\alpha = (2+2\mu)/(5+4\mu)$, $\beta = 1/(5+4\mu)$.

In summary, the Smoluchowski theory provides a simple and surprisingly comprehensive account for the kinetics of heterogeneous single-species annihilation, both in the mean-field limit and in 1D.

1.3.2 Ballistic annihilation

As mentioned in Sec. 1.1, ballistically driven reactions are relatively unexplored in spite of their relative simplicity and apparent richness. In such systems, particles move with their initial velocities until a reaction occurs, so that the initial condition determines the time dependence. Past work has primarily been on the '±' model in 1D [33], where each particle velocity is either $+v_0$ or $-v_0$ with equal probability. Part of the interest in this reaction is its equivalence to the polynuclear growth model (Fig. 1.4) [34]. This is a model of evolving 'positive' and 'negative' terraces which move at constant speed and annihilate when oppositely oriented terraces meet.

For the ± ballistic reaction, the concentration decays as $c(t) \propto \sqrt{c(0)/vt}$. In analogy with the diffusion-controlled case $A + B \to 0$, this result can be understood by considering density fluctuations in a domain of length ℓ. In such a region, there will typically be an imbalance $\delta n \simeq \sqrt{c(0)\ell}$ in the number of right-moving and left-moving particles. After a time $t = \ell/v$, only this residual fluctuation will remain and the concentration will be of order $c(t) \simeq \delta n/\ell$. Expressing ℓ in terms of t then gives $c(t) \propto t^{-1/2}$. In the following, extensions to more general velocity distributions will be presented.

1. Continuous velocity distribution

For a continuous zero mean initial velocity distribution, $P(v, t = 0)$, basic quantities that characterize the reaction include the concentration, $c(t) =$

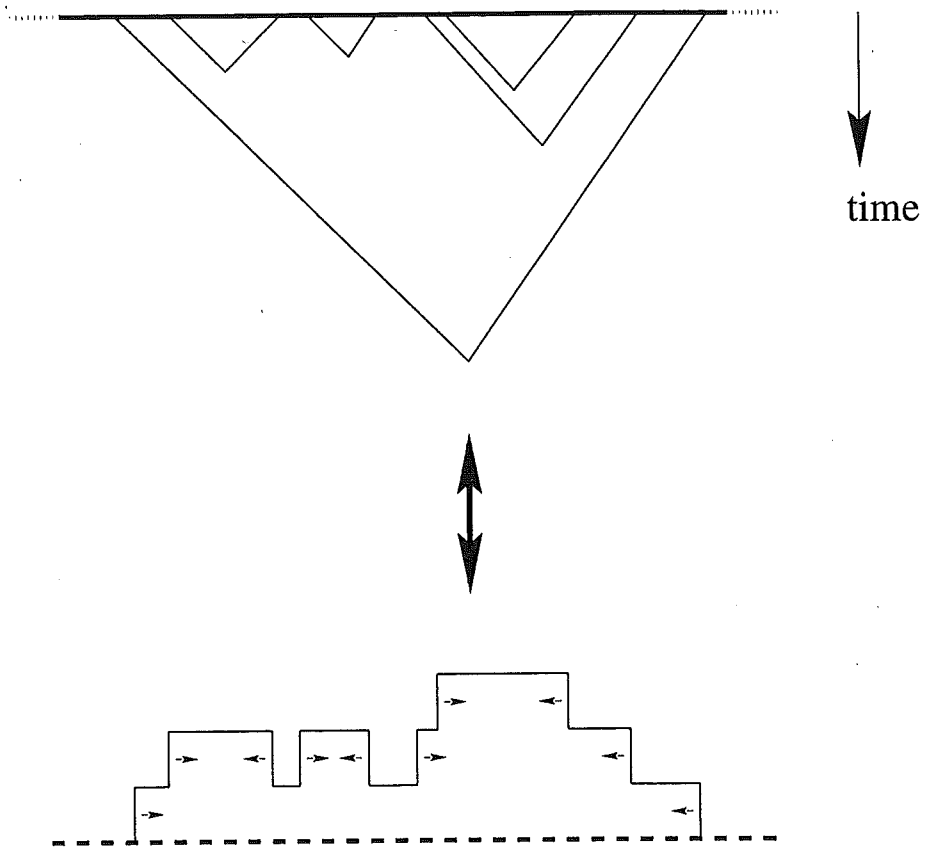

Fig. 1.4. Schematic illustration of the equivalence of the space-time evolution of the deterministic ± model and the polynuclear growth model of surface growth. The initial conditions of the two systems are equivalent. The velocities of the terraces in the polynuclear growth model representation are indicated.

$\int dv P(v,t) \sim t^{-\alpha}$ and the rms velocity, $v_{\rm rms} = [\int dv\, v^2 P(v,t)/c(t)]^{1/2} \sim t^{-\beta}$. From a mean-free path argument, the time between collisions for particles of (fixed) radius r and speed $v_{\rm rms}$ with concentration c is $t \sim 1/(c v_{\rm rms} r^{d-1})$, or $c v_{\rm rms} \propto t^{-1}$, leading to the scaling relation $\alpha + \beta = 1$. Since the particle lifetime is proportional to $1/v$, faster particles tend to annihilate more quickly, and the typical velocity decays in time. This parallels the behavior found in heterogeneous diffusion-controlled single-species annihilation.

The evolution of the velocity distribution in 1D is described by the Boltzmann equation [35]

$$\frac{\partial P(v,t)}{\partial t} = -kP(v,t) \int_{-\infty}^{\infty} dv' \, |v - v'| \, P(v',t). \tag{1.18}$$

In spite of its mean-field character, (1.18) and its d-dimensional generalization give a quantitatively accurate description of the decay kinetics. This rate equation can again be analyzed by scaling. Assuming that the velocity distribution has the scaled form $P(v,t) \simeq t^{\beta-\alpha}\Phi(vt^{\beta})$, substituting this into (1.18), and demanding consistency of both sides of the resulting equation leads to the exponent relation $\alpha+\beta=1$ and a nonlinear integro-differential equation for $\Phi(z)$. As in heterogeneous diffusion-controlled $A+A\to 0$, the limiting behaviors of the scaling function can be extracted by a combination of asymptotic and scaling arguments. For an initial velocity distribution of the form $P(v,t=0)\propto |v|^{\mu}$ for small v, $\Phi(z)$ has the asymptotic forms $\Phi(z)\sim z^{\mu}$ as $z\to 0$, and $\Phi(z)\sim e^{-|z|/\beta}$ as $z\to\infty$. If one makes an ansatz that the full scaling function is the product $|z|^{\mu}e^{-|z|/\beta}$, then the governing equation for $\Phi(z)$ yields $\beta=1/(3+2\mu)$. As a result, α and β can take on any value between 0 and 1 as μ is varied, subject to $\alpha+\beta=1$. Notice that when the concentration decays relatively quickly, $\alpha\lesssim 1$, the typical velocity decays slowly, and vice versa. It is gratifying, although somewhat surprising in the light of the approximations involved, that the Boltzmann equation predictions are in relatively good agreement with simulations [35].

2. Discrete three-velocity distribution

Unusual and incompletely understood phenomena arise for discrete velocity distributions. A generic illustration is the trimodal distribution $P(v,t=0)=p_+\delta(v-1)+p_0\delta(v)+p_-\delta(v+1)$, with $p_++p_0+p_-=1$ [36]. In the mean-field limit, the kinetics of the symmetric system with $p_+=p_-\equiv p_{\pm}$ is described by the rate equations, $\dot{c}_{\pm}=-c_0c_{\pm}-2c_{\pm}^2$, $\dot{c}_0=-2c_0c_{\pm}$, with corresponding asymptotic behaviors

$$c_{\pm}(t)\sim\frac{1}{2}c_0(\infty)\,e^{-c_0(\infty)t},\qquad c_0(t)\sim c_0(\infty)\exp\left[e^{-c_0(\infty)t}\right]. \tag{1.19}$$

Here $c_0(\infty)=c_0(t=0)\;e^{-2c_{\pm}(0)/c_0(0)}$. Thus the mobile particles decay exponentially in time, while a residue of stationary particles always remains whose concentration is vanishingly small if the initial concentration is relatively small.

However, from both nonrigorous approaches and an exact solution for the special case $p_+=p_-$ [37,38], rather different behavior occurs in 1D. As a function of p_0, a transition occurs from a regime where the stationary particles persist, for $p_0>1/4$, to a regime where $c_0(t)\sim t^{-1}$ and $c_{\pm}(t)^{-1/2}$, for $p_0<1/4$. At a 'tricritical' point located at $p_0=1/4$, the concentrations of the mobile and stationary species decay as $t^{-2/3}$. While all asymptotic information is contained in the exact solution, the qualitative approaches

are still instructive. The location of the tricritical point may be found by a stoichiometric argument [36]. Since half the stationary particles react with + particles, the fraction of + particles available to react with − particles is $p_+ - \frac{1}{2}p_0$. This is proportional to the number of $+-$ annihilation events per unit length, $\mathcal{N}_{+-}$. Similarly, the relative number $\mathcal{N}_{0-}$ of $0-$ annihilation events per unit length equals $\frac{1}{2}p_0$. It is reasonable to assume that the relative number of annihilation events is proportional to the relative velocities of the collision partners, so that $\mathcal{N}_{+-}/\mathcal{N}_{0-} = 2$. Combining the resulting relation, $p_+ - \frac{1}{2}p_0 = p_0$, with the normalization condition, $2p_+ + p_0 = 1$, gives the exact location of the tricritical point: $p_0 = 1/4$, $p_\pm = 3/8$.

The two different exponent values for the decay of $c_0(t)$ and $c_\pm(t)$ in the case $c_0(0) < 1/4$ can also be understood by a probabilistic argument that applies in the limit $c_0(0) \to 0$. For an infinitesimal concentration of stationary 'impurities', the moving particles react among themselves with overwhelming probability and the background system reduces to the $\pm$ model, for which $c_\pm(t) \sim t^{-1/2}$. On the other hand, a stationary particle survives only if it is not annihilated by moving particles incident from either direction. Since the probabilities of each of these two events are independent, it follows that $c_0(t) \sim [c_\pm(t)]^2 \sim t^{-1}$ in the limit $c_0(0) \ll c_\pm(0)$.

When the initial concentrations of the three species are arbitrary, there are three 'phases'—regions of the phase diagram where a single species persists in the long-time limit (Fig. 1.5). As just discussed, the stationary species decays relatively quickly along the boundary between the + phase (where right-moving particles persist) and the − phase. The complementary situation of the decay of −'s along the $+0$ phase boundary also exhibits peculiar characteristics. For simplicity, consider an infinitesimal concentration of −'s in a background of equal concentrations of 0's and +'s. By a Galilean transformation, this is equivalent to 'fast impurities' in a symmetric $\pm$ background. A Lifshitz-type argument suggests that the survival probability of this fast impurity decays slower than exponentially but faster than a power law in time.

The basis of this argument is to consider a subset of configurations which give the dominant contribution to the impurity survival probability $S(t)$, but which are sufficiently simple to evaluate [36]. For the impurity to survive to time t, the background $\pm$ particles must annihilate *only* among themselves up to this time. On a space-time diagram, the dominant contribution to $S(t)$ stems from a sequence of ever larger self-annihilation triangles that just 'miss' the impurity world line (Fig. 1.6). The base of the nth triangle $x_n \propto [(v_0+1)/(v_0-1)]^n \equiv \beta^n$ and the number of triangles in this self-annihilation sequence up to time t is $N \simeq \ln t/\ln\beta$. Because the probability

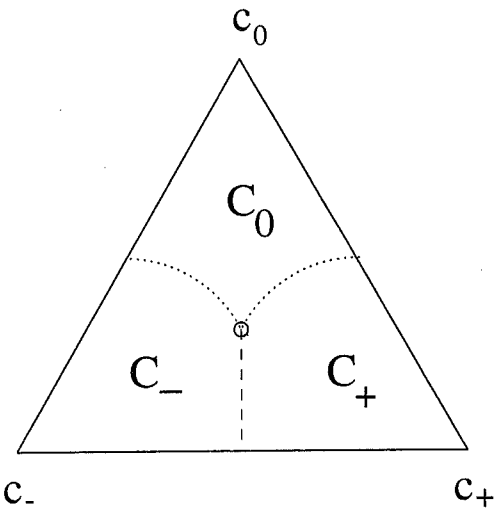

Fig. 1.5. Phase diagram of the 1D three-velocity model in the triangle defined by the relative concentrations of the three species. Along the broken line, $c_\pm(t) \sim t^{-1/2}$, while $c_0(t) \sim t^{-1}$. At the point marked by the small circle, $c_\pm(0) = 3/8$, $c_0(0) = 1/4$, all species decay as $t^{-2/3}$. Along the dotted lines, the nature of the decay is unknown, except very close to the extrema that correspond to the 'fast impurity' problem (see below). The symbols inside the triangle indicate the concentrations of the species dominant in the long-time limit.

of a particle annihilating with its nth neighbor asymptotically decreases as $n^{-3/2}$ [33], a self-annihilation triangle of base x_n occurs with probability $x_n^{-3/2}$. Finally $S(t)$ is the product of the occurrence probabilities of this self-annihilation triangle sequence,

$$S(t) \sim \prod_{n=1}^{\ln t/\ln\beta} (2x_0\beta^n)^{-3/2} \sim \exp[-3\ln^2 t/(4\ln\beta)]. \qquad (1.20)$$

This result has been confirmed numerically.

A natural continuation of the above line of modeling is to the four-velocity model with particle velocities $\pm v_1$ and $\pm v_2$, $v_2 > v_1$, and with relative concentrations c_1 and c_2. While the rate equations predict that the faster species decays as t^{-v_2/v_1} and the slower species decays as t^{-1}, the 1D system exhibits tricritical behavior reminiscent of the three-velocity model. Namely, there exists an initial condition, which depends on v_2/v_1, for which all four species appear to decay at the same power-law rate of approximately $t^{-0.72}$. A comprehensive understanding of these and more general discrete velocity systems is still lacking.

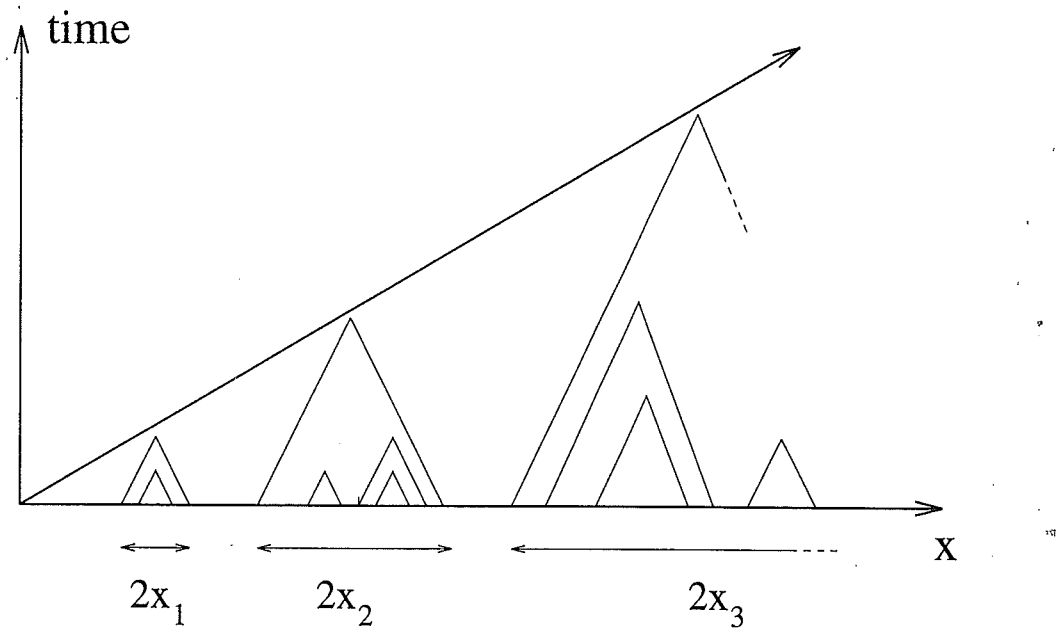

Fig. 1.6. World line of a fast impurity in a background of equal concentrations of ± particles. Successive triangles of self-annihilating background particles are indicated.

1.3.3 The stochastic ± model

As a final example of a single-species annihilation process that exhibits unusual kinetics, consider the 'stochastic' ± model, where particles execute biased diffusion with fixed bias (either right or left) for each particle [36]. For the deterministic ± model, particles with the same velocity never meet, by definition. However, in the stochastic ± model, the superimposed diffusion permits same-velocity particles to annihilate, a mechanism that leads to surprising behavior. This can be determined by dimensional analysis. If the particle diffusion coefficient is D, then the stochastic ± model is fully characterized by the initial concentration c_0, the velocity v_0, and D. From these parameters, the only variable combinations with the dimensions of concentration are, c_0, $1/(v_0 t)$, and $1/\sqrt{Dt}$. From basic considerations about the nature of the decay, the time-dependent concentration is anticipated to have the form

$$c(t) \propto (c_0)^{\mu} \left(\frac{1}{v_0 t}\right)^{\nu} \left(\frac{1}{\sqrt{Dt}}\right)^{1-\mu-\nu}. \tag{1.21}$$

The exponents μ and ν can be determined by requiring that $c(t)$ matches with (a) the diffusion-limited result $c(t) \to (Dt)^{-1/2}$ when $t < \tau_v \simeq D/v_0^2$, the crossover time below which drift can be ignored, and (b) the ballistic

result $c(t) \to (c_0/v_0 t)^{1/2}$ for $t < \tau_D \simeq 1/(Dc_0^2)$, which is the time for adjacent particles to meet by diffusion. This matching gives

$$c(t) \sim \left(\frac{1}{v_0 t}\right)^{1/2} \left(\frac{1}{\sqrt{Dt}}\right)^{1/2} \propto t^{-3/4}. \tag{1.22}$$

Interestingly, the concentration decays as $t^{-1/2}$ for both the diffusion-limited and the ballistically limited reactions, but the combination of both mechanisms leads to a faster, $t^{-3/4}$, decay.

1.3.4 Ballistic aggregation

Another intriguing class of ballistically driven reactions is irreversible aggregation, $A_i + A_j \to A_{i+j}$, where A_i denotes a species with mass i. In the situation where each aggregation event conserves momentum, a scaling approach [39] shows that the cluster concentration $c(t) \equiv \sum_{k=1}^{\infty} c_k(t)$, where $c_k(t)$ is the concentration of clusters of mass k, decays as $c(t) \sim t^{-2d/(d+2)}$. Numerical simulations indicate that this mean-field prediction holds even in 1D. However, there are significant discrepancies in microscopic aspects of the reaction in 1D [40]. For example, the scaling approach gives $c_k(t) \sim \exp(-\text{constant} \times t^{1/3})$ for cluster mass k much less than the typical mass, while a Lifshitz tail argument gives $c_k(t) \sim t^{-1}$, a result that has been verified numerically [40].

The result for the cluster concentration can be reproduced by a mean-free-path argument that parallels the earlier 'microscopic' formulation of the rate equation. Consider a monomer-only initial condition in which each particle has the same speed but random direction. The momentum of an aggregate of mass m is proportional to $m^{1/2}$, since it is the sum of m random momenta. Consequently, the time between collisions at any stage of the reaction is $\Delta t \simeq 1/(cv\sigma)$, where c is the concentration, $v = p/m \propto m^{-1/2}$ is the typical velocity, and σ is the cross-section. In this time interval, the concentration decrement is of order $\Delta c \sim -c$. Thus $\Delta c/\Delta t \simeq -c/[1/(cv\sigma)]$. For a typical aggregate with mass $m \propto 1/c$, the r.h.s. can be rewritten in terms of the concentration only, using $v \sim c^{1/2}$ and $\sigma \sim c^{-(d-1)/d}$, leading to $c(t) \sim t^{-2d/(d+2)}$.

In the following, a complementary problem of ballistic aggregation, which models traffic flow on a 1D road with no passing, will be discussed [41]. Consider zero-size cars that move ballistically in one direction. We suppose that whenever a faster car or cluster overtakes a slower object, the larger final cluster assumes the velocity of the overtaken object. This reaction can be schematically represented as $A_{m_1,v_1} + A_{m_2,v_2} \to A_{m_1+m_2,\min\{v_1,v_2\}}$, where

A_{m_i,v_i} denotes a cluster with velocity v_i and which contains m_i cars. Scaling approaches, together with the statistical properties of the minimal random variable of a sample, determine basic system observables.

Let m and v be the typical cluster mass (or number of cars) and cluster velocity at time t. Without loss of generality, the minimal car velocity may be taken to be zero. The typical distance, ℓ, between clusters therefore grows as $\ell \sim vt$. Since the typical cluster mass is proportional to the typical intercluster distance, one also has $m \sim \ell \sim vt$. To find the typical velocity, one has to relate the cluster size to its velocity. Such a relation may be found exactly for a 'one-sided' problem in which the 'leading' car is placed at $x = 0$ and other cars are *only* in the domain $x < 0$. This leading car ultimately forms a cluster that includes all *consecutive* cars to its left whose initial velocities are larger than v. The probability that there are exactly k such cars equals $\Pi_-\Pi_+^k$, where $\Pi_+ = 1 - \Pi_- = \int_v^\infty P(v', t = 0)dv'$ is the probability that a car has velocity larger than v. The average number of cars in the cluster that ultimately forms is therefore given by $\langle m(v)\rangle = \sum_{k=1}^\infty k\Pi_-\Pi_+^k = \Pi_+/\Pi_-$.

For a power-law small-velocity tail of the initial velocity distribution, $P(v, t = 0) \propto v^\mu$ for $v \ll 1$ (with $\mu > -1$ for normalizability), $\langle m(v)\rangle \cong v^{-1-\mu}$. Under the assumption that this 'one-sided' result also applies to the original 'two-sided' problem and also using $m \sim vt$ one obtains

$$m \sim c^{-1} \sim t^\alpha, \quad \text{with} \quad \alpha = \frac{\mu+1}{\mu+2}; \qquad v \sim t^{-\beta}, \quad \text{with} \quad \beta = \frac{1}{\mu+2}. \quad (1.23)$$

In analogy with ballistic annihilation with continuous velocities, the exponent relation $\alpha + \beta = 1$ is a consequence of the relation $c \sim 1/vt$.

An extension of the above reasoning allows one to solve for the mass and velocity distributions in the traffic model. As an illustration, consider the survival probability of a given car with velocity v, $S(v, t)$. Here 'survival' means that the car does not overtake traffic, but if overtaken still 'survives', i.e., a survivor leads a cluster of size $m \geq 1$. The survival probability can be found by considering the possible collisions of a car with initial velocity v and position x with slower cars. A collision with a slower v'-car does not occur up to time t if the interval $[x, x + (v - v')t]$ does not include the v'-car. For a continuous initial velocity distribution and a Poissonian initial spatial distribution, the probability that the v'-car is not in the interval $[x, x + (v - v')t]$ is $\exp\{-dv'\, P(v', t = 0)\,(v - v')\,t\}$. The probability that the initial car survives up to time t equals the product of these pair survival

factors for every $v' < v$. Hence,

$$S(v,t) = \exp\left\{-t\int_0^v dv'(v-v')\,P(v',t=0)\right\}, \tag{1.24}$$

and the cluster velocity distribution is $P(v,t) = P(v,t=0)\,S(v,t)$.

For $P(v,t=0) \sim v^\mu$ as $v \to 0$, (1.24) gives the asymptotic velocity distribution as

$$P(v,t) \propto v^\mu \exp\left\{-\text{constant} \times t v^{\mu+2}\right\}. \tag{1.25}$$

This universal form validates the scaling assumption that the asymptotic decay and the shape of the limiting distribution are determined solely by the exponent μ that characterizes the low-velocity tail of $P_0(v)$. From (1.25), the total concentration, $c(t) = \int_0^\infty dv\,P(v,t)$, and the average cluster velocity $\langle v(t)\rangle = \int dv\,vP(v,t)/\int dvP(v,t)$ are found to agree with (1.23). Extensions of this reasoning determine the complete distribution of clusters of mass m and velocity v.

1.4 Summary

The scaling approach is a simple yet powerful tool for analyzing the kinetics of simple reaction processes. In diffusion-limited two-species annihilation, a scaling analysis leads to an understanding of the coarsening mosaic of A and B domains from the initial density fluctuations. A relatively simple-minded adaptation of the rate equation approach reveals that the spatial distribution of reactants involves a multiplicity of scales that originates from the existence of a new length, ℓ_{AB}, the separation between AB nearest-neighbor pairs. Consideration of the density profile of a single domain provides a revealing picture of the 'internal' spatial organization of reactants. Scaling approaches are also useful in elucidating some of the unexpected features of two-species annihilation when the reactants undergo driven diffusion.

Although many aspects of 1D single-species reaction kinetics are exactly solvable, scaling approaches provide a relatively simple route to a comprehensive understanding. An attractive feature of the scaling formulation is that the apparently disparate processes of diffusion-controlled and ballistically controlled reactions may be analyzed in essentially identical manners. Although quantitative details depend on the specifics of a particular reaction, qualitative features are universal and are captured by a scaling description.

One intriguing aspect of single-species reactions, for which scaling appears to have limited utility, is the case of discrete diffusivity or velocity distributions. For example, in diffusive $A + A \to 0$ in 1D with an infinitesimal fraction of immobile particles in a background of equally mobile particles the density of the immobile particles decays as $t^{-3/8}$, compared to a decay of $t^{-1/2}$ for the background particles. Variations of this type of problem may be fruitful areas for additional investigation. For ballistically driven annihilation with three different velocity species in 1D, a wide range of kinetics arises, either 'critical', with two species decaying as $t^{-1/2}$ and the minority species decaying more quickly, or 'tricritical', where all three species decay as $t^{-2/3}$. While this latter behavior has been found by an exact solution, an intuitive understanding is still lacking and the full range of phenomenology appears ripe for further exploration. Finally, for combined ballistic and diffusive reactant motion, the concentration decays more rapidly than in the limiting situations where only one transport mechanism is operative. This interesting behavior can be accounted for by dimensional analysis. However, a microscopic theory has yet to be developed.

The author thanks Eli Ben-Naim, Slava Ispolatov, Paul Krapivsky, and François Leyvraz for pleasant collaborations that formed the basis of much of the work reviewed here. His initial work in this field was performed in collaboration with the late Kiho Kang who he still fondly remembers. The author is also grateful to Dani ben-Avraham, Charlie Doering, and Vladimir Privman for many instructive discussions, and to Paul Krapivsky for a critical reading of this chapter. Finally, he is grateful to the granting agencies that provided financial support for his work, including the ARO (through grant DAAH04-93-G-0021), the NSF (through grants INT-8815438 and DMR-9219845), and the Donors of The Petroleum Research Fund, administered by the American Chemical Society.

References

[1] A. A. Ovchinnikov and Ya. B. Zel'dovich, *Chem. Phys.* **28**, 215 (1978); S. F. Burlatskii and A. A. Ovchinnikov, *Russ. J. Phys. Chem.* **52**, 1635 (1978).

[2] D. Toussaint and F. Wilczek, *J. Chem. Phys.* **78**, 2642 (1983).

[3] K. Kang and S. Redner, *Phys. Rev. Lett.* **52**, 955 (1984); *Phys. Rev.* A**32**, 435 (1985).

[4] K. Lee and E. J. Weinberg, *Nucl. Phys.* B**246**, 354 (1984).

[5] P. Meakin and H. E. Stanley, *J. Phys.* A**17**, L173 (1984).

[6] G. Zumofen, A. Blumen and J. Klafter, *J. Chem. Phys.* **82**, 3198 (1985).

[7] L. W. Anacker and R. Kopelman, *Phys. Rev. Lett.* **58**, 289 (1987); D. ben-Avraham and C. R. Doering, *Phys. Rev.* A**37**, 5007 (1988); K. Lindenberg, B.

J. West and R. Kopelman, *Phys. Rev. Lett.* **60**, 1777 (1988); E. Clément, L. M. Sander and R. Kopelman, *Phys. Rev.* A**39**, 6455 (1989).

[8] M. Bramson and J. L. Lebowitz, *Phys. Rev. Lett.* **61**, 2397 (1988); M. Bramson and J. L. Lebowitz, *J. Stat. Phys.* **62**, 297 (1991); M. Bramson and J. L. Lebowitz, *J. Stat. Phys.* **65**, 941 (1991).

[9] B. P. Lee and J. L. Cardy, *Phys. Rev.* E**50**, 3287 (1994); B. P. Lee and J. L. Cardy, *J. Stat. Phys.* **80**, 971 (1995).

[10] L. Gálfi and Z. Racz, *Phys. Rev.* A**38**, 3151 (1988); Y.-E. L. Koo and R. Kopelman, *J. Stat. Phys.* **65**, 893 (1991); S. Cornell, M. Droz and B. Chopard, *Phys. Rev.* A**44**, 4826 (1991); M. Araujo, S. Havlin, H. Larralde and H. E. Stanley, *Phys. Rev. Lett.* **68**, 1791 (1992); H. Larralde, M. Araujo, S. Havlin and H. E. Stanley, *Phys. Rev.* A**46**, 855 (1992); E. Ben-Naim and S. Redner, *J. Phys.* A**25**, L575 (1992); S. Cornell and M. Droz, *Phys. Rev. Lett.* **70**, 3824 (1993); P. L. Krapivsky, *Phys. Rev.* E**51**, 4774 (1995).

[11] For recent reviews on two-species annihilation see, e.g., Ya. B. Zel'dovich and A. S. Mikhailov, *Sov. Phys. Usp.* **30**, 23 (1988); V. Kuzovkov and E. Kotomin, *Rep. Prog. Phys.* **51**, 1479 (1988); R. Kopelman, *Science* **241**, 1620 (1988); A. S. Mikhailov, *Phys. Reports* **184**, 307 (1989); A. A. Ovchinnikov, S. F. Timashev and A. A. Belyy, in *Kinetics of Diffusion Controlled Chemical Processes* (Nova Science Publishers, 1990); S. Redner and F. Leyvraz, *Fractals and Disordered Systems*, Vol. **2**, S. Havlin and A. Bunde, eds. (Springer, Heidelberg, 1994).

[12] M. V. Smoluchowski, *Z. Phys. Chem.* **92**, 215 (1917); S. Chandrasekhar, *Rev. Mod. Phys.* **15**, 1 (1943).

[13] See, e.g., G. H. Weiss and R. J. Rubin, *Adv. Chem. Phys.* **52**, 363 (1983), and references therein.

[14] C. R. Doering and D. ben-Avraham, *Phys. Rev.* A**38**, 3035 (1988); D. ben-Avraham, M. A. Burschka and C. R. Doering, *J. Stat. Phys.* **60**, 695 (1990).

[15] F. Leyvraz and S. Redner, *Phys. Rev. Lett.* **66**, 2168 (1991); *Phys. Rev.* A**46**, 3132 (1992). The importance of interparticle distributions in two-species annihilation was apparently first raised in P. Argyrakis and R. Kopelman, *Phys. Rev.* A**41**, 2121 (1990).

[16] See, e.g., L. D. Landau and E. M. Lifshitz, *Quantum Mechanics* (Pergamon Press, New York, 1977).

[17] S. A. Janowsky, *Phys. Rev.* E**51**, 1858 (1995).

[18] I. Ispolatov, P. L. Krapivsky and S. Redner, *Phys. Rev.* E**52**, 2540 (1995).

[19] S. A. Janowsky, *Phys. Rev.* E**52**, 2535 (1995).

[20] D. C. Torney and H. M. McConnell, *Proc. Roy. Soc. London* A**387**, 147 (1983); D. C. Torney and H. M. McConnell, *J. Phys.* C**87**, 1941 (1983).

[21] A. A. Lushnikov, *Sov. Phys. JETP* **64**, 811 (1986).

[22] Z. Rácz, *Phys. Rev. Lett.* **55**, 1707 (1985); J. G. Amar and F. Family, *Phys. Rev.* A**41**, 3258 (1990); V. Privman, *J. Stat. Phys.* **69**, 629 (1992).

[23] P. Argyrakis and R. Kopelman, *Phys. Rev.* A**41**, 2113 (1990).

[24] T. J. Cox and D. Griffeath, *Ann. Prob.* **14**, 347 (1986). For general results about the voter model, see, e.g., R. Durrett, *Lecture Notes on Particle Systems and Percolation* (Wadsworth and Brooks/Cole, Pacific Grove, CA, 1988).

[25] M. Bramson and D. Griffeath, *Z. Wahrsch. verw. Gebiete* **53**, 183 (1980).

[26] J. L. Spouge, *Phys. Rev. Lett.* **60**, 873 (1988).

[27] D. J. Balding, *J. Appl. Phys.* **25**, 733 (1988); D. J. Balding and N. J. B. Green, *Phys. Rev.* A**40**, 4585 (1989).

[28] P. L. Krapivsky, E. Ben-Naim and S. Redner, *Phys. Rev.* E**50**, 2474 (1994).

[29] B. Derrida, A. J. Bray and C. Godréche, *J. Phys.* A**27**, L357 (1994); D. Stauffer, *J. Phys.* A**27**, 5029 (1994); J. L. Cardy, *J. Phys.* A**28**, L19 (1995); B. Derrida, *J. Phys.* A**28**, 1481 (1995).
[30] B. Derrida, V. Hakim and V. Pasquier, *Phys. Rev. Lett.* **75**, 751 (1995).
[31] F. Leyvraz, unpublished; D. ben-Avraham, *J. Chem. Phys.* **88**, 941 (1988); M. E. Fisher and M. P. Gelfand, *J. Stat. Phys.* **53**, 175 (1988); M. Bramson and D. Griffeath, in *Random Walks, Brownian Motion and Interacting Particle Systems: A Festschrift in Honor of Frank Spitzer*, R. Durrett and H. Kesten, eds. (Birkhauser, 1991), and references therein.
[32] For a pedagogical account see, e.g., P. Krapivsky and S. Redner, *Am. J. Phys.* **64**, 546 (1996). References to original literature are contained therein.
[33] Y. Elskens and H. L. Frisch, *Phys. Rev.* A**31**, 3812 (1985); J. Krug and H. Spohn, *Phys. Rev.* A**38**, 4271 (1988).
[34] D. Kashchiev, *J. Crystal Growth* **40**, 29 (1977); C. H. Bennett, M. Büttiker, R. Landauer and H. Thomas, *J. Stat. Phys.* **24**, 419 (1981); M. C. Bartelt and J. W. Evans, *J. Phys.* A**26**, 2743 (1993).
[35] E. Ben-Naim, S. Redner and F. Leyvraz, *Phys. Rev. Lett.* **70**, 1890 (1993).
[36] P. Krapivsky, S. Redner and F. Leyvraz, *Phys. Rev.* E**51**, 3977 (1995). Note that a version of ballistic annihilation with a trimodal velocity distribution was introduced by W. S. Sheu, C. van den Broeck and K. Lindenberg, *Phys. Rev.* A**43**, 4401 (1991). However, the collision rules of this model were formulated to give behavior similar to that of the two-velocity model.
[37] J. Piasecki, *Phys. Rev.* E**51**, 5535 (1995).
[38] M. Droz, L. Frachebourg, J. Piasecki and P.-L. Rey, *Phys. Rev. Lett.* **75**, 160 (1995); *Phys. Rev.* E**51**, 5541 (1995).
[39] G. F. Carnevale, Y. Pomeau and W. R. Young, *Phys. Rev. Lett.* **64**, 2913 (1990).
[40] Y. Jiang and F. Leyvraz, *J. Phys.* A**26**, L179 (1993).
[41] E. Ben-Naim, P. L. Krapivsky and S. Redner, *Phys. Rev.* E**50**, 822 (1994).